

1 SUPPLEMENTAL METHODS

2

3 Cell culture

4 Hematopoietic stem and progenitor cells (HSPCs) (#2M-101C Lonza) were cultured in IMDM
5 (Gibco, life technologies) supplemented with 2.5 % BSA (PAN-Biotech GmbH), 1X ITS-G
6 (Gibco, life technologies), 20 μ M β -Mercaptoethanol (Acros Organics), 1mM UltraGlutamine-
7 I (Lonza), 50 μ g/ml Gentamicin (Acros Organics), 10 μ g/ml Ciprofloxacin (Acros Organics),
8 50 μ M 2P-Ascorbic Acid (Sigma-Aldrich), 1 μ g/mL Heparin (AppliChem GmbH), 0.5 \times
9 Synthechol (Sigma-Aldrich), 50 ng/mL SCF (Immunotools), 50 ng/ml FLT3L (Immunotools),
10 25 ng/ml TPO (Immunotools) and 35 nM UM171 (Selleckchem).

11

12 Ex vivo T-lymphoid differentiation culture assay

13 LSK cells (Lin- Sca-1+ c-kit+) from a PU.1 knockout mouse model were transduced to stably
14 express a human PU.1 gene including all regulatory elements¹. For in vitro T-lymphoid
15 coculture, 1×10^4 stromal cells were plated into each well of 24-well plates two days before
16 plating of stem/progenitor cells. Sorted LSK were infected with small-hairpin RNA knockdown
17 of PU.1 asRNA (shPU.1as) or by scrambled control (shControl). Infected stem/progenitor cells
18 were added to the OP9-DL1 stromal cells lines as previously described² at Day 0. Cells were
19 cultured in α -MEM (Invitrogen) supplemented with 10% FCS. Flt3-L, SCF and IL-7
20 (PeproTech). At Day 14-17 cultures of stromal cells and hematopoietic cells were harvested
21 using 0.53 mM EDTA/PBS (pH 7.4). CD45 and DAPI were used to distinguish viable blood
22 cells from OP9-DL1 stroma.

23

24 RNA isolation and Northern Analysis

25 RNA isolation, electrophoresis, transfer and hybridization were carried out as described³.
26 Polyadenylated mRNAs were selected according to the MicroPoly(A)PuristTM purification kit
27 (Ambion). Preparation of separate nuclear and cytoplasmic fractions was performed according
28 to the ParisTM kit (Ambion). Northern Quantitative analysis was performed on the Storm
29 Phosphorimager. The antisense-specific probe - mixture of two cloned PCR products are
30 described in Supplemental Table2.

31

32 ATAC-seq analysis

33 Raw .fastq files were adapter trimmed using *Trim Galore!* software
34 (http://www.bioinformatics.babraham.ac.uk/projects/trim_galore/) and aligned to GRCh37

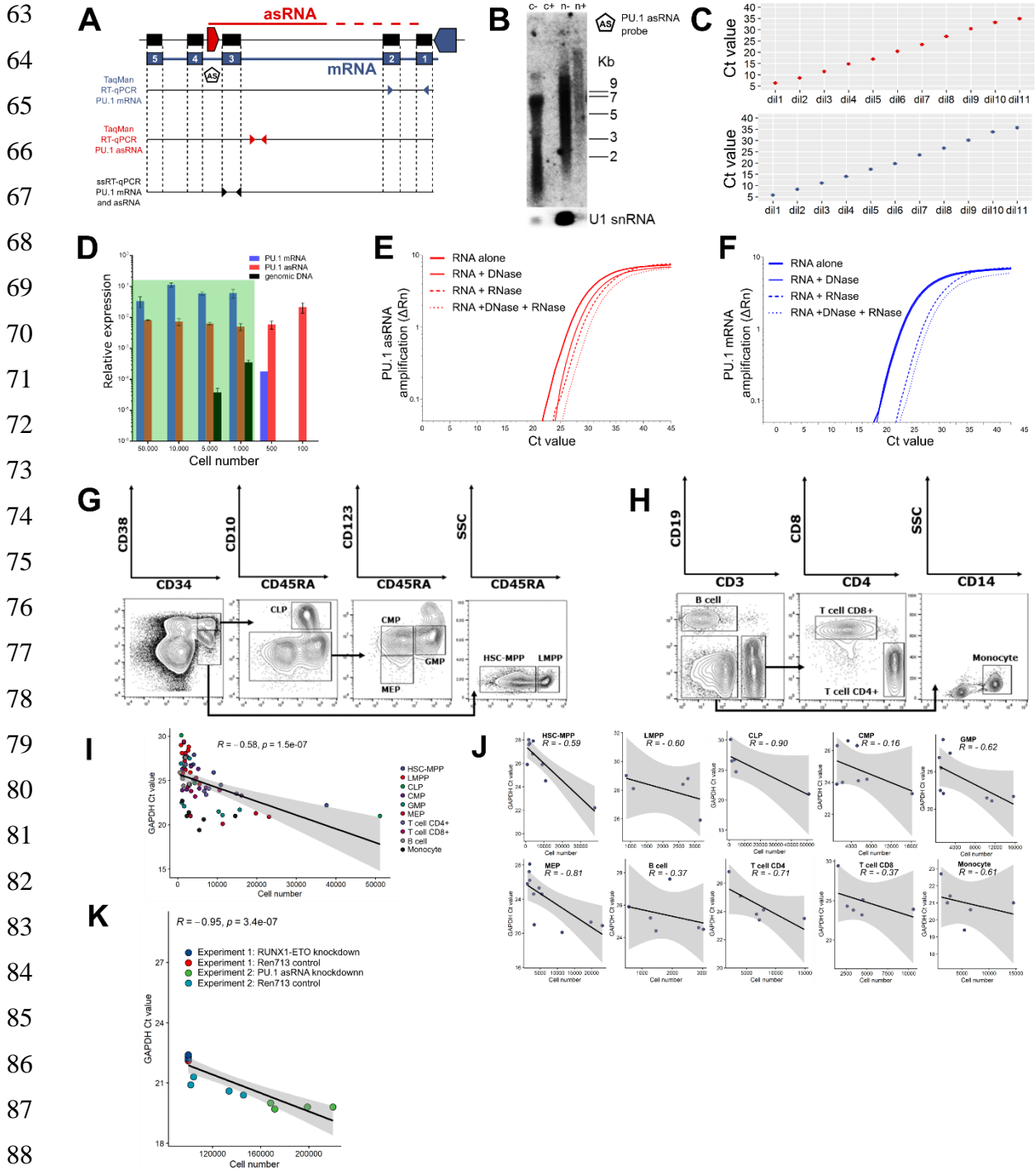
35 using bowtie2⁴. Reads corresponding to mitochondrial DNA were removed using samtools
36 (samtools view -@ 20 -h \$i | grep -v MT | samtools sort)⁵. Picard tools
37 (<http://broadinstitute.github.io/picard>) were used to mark duplicate reads arising during PCR as
38 artefacts of the library preparation procedure followed by duplicate read and multimapper
39 removal by samtools (samtools view -@ 20 -h -b -q 30 -F 1024). Bigwig files were generated
40 using deepTools, peaks were called by MACS2 and quantified using the R package diffbind⁶.
41 Intensity values were adjusted to the PU.1 -17kb URE; a quantification inferior to 1:8th of both
42 AsPr and PrPr was used as a filter for outliers. Raw ATAC-seq data were deposited in the
43 ArrayExpress database (Accession ID: E-MTAB-9021).

44 **RERERENCES**

- 45 1. Leddin M, Perrod C, Hoogenkamp M, et al. Two distinct auto-regulatory loops operate
46 at the PU.1 locus in B cells and myeloid cells. *Blood*. 2011;117(10):2827-2838.
- 47 2. Schmitt TM, Zúñiga-Pflücker JC. Induction of T cell development from hematopoietic
48 progenitor cells by delta-like-1 in vitro. *Immunity*. 2002;17(6):749-756.
- 49 3. Maniatis T, Fritsch EF, Sambrook J. Molecular cloning: a laboratory Manual. Cold
50 Spring Harbor, New York: Cold Spring Harbor Laboratory Press; 1982.
- 51 4. Langmead B, Salzberg SL. Fast gapped-read alignment with Bowtie 2. *Nat Methods*.
52 2012;9(4):357-359.
- 53 5. Li H. A statistical framework for SNP calling, mutation discovery, association
54 mapping and population genetical parameter estimation from sequencing data. *Bioinformatics*.
55 2011;27(21):2987-2993.
- 56 6. Ross-Innes CS, Stark R, Teschendorff AE, et al. Differential oestrogen receptor
57 binding is associated with clinical outcome in breast cancer. *Nature*. 2012;481(7381):389-
58 393.
- 59
60

61 SUPPLEMENTAL FIGURES

62 Supplemental Figure 1



63 Supplemental Figure 1. **PU.1 quantification assay validation, hematopoietic population**
 64 **isolation for PU.1 transcript quantification and hematopoietic transcription factor**
 65 **mobilization during thymic differentiation.** (A) Schematic representation of the PU.1 locus
 66 with the antisense promoter (AsPr, red arrow box) and proximal (PrPr, blue arrow box),
 67 respectively regulating the transcription of the antisense RNA (asRNA, red line) and the coding

95 mRNA (blue line, exon number 1-5). Forward and reverse primer (left and right arrows) pair
96 localization each PU.1 transcript quantification using RT-qPCR or strand-specific RT-qPCR
97 (ssRT-qPCR). Black pentagon arrow shows PU.1 asRNA probe for Northern blot analysis.
98 Colors used in this schematic are consistent throughout the figure. **(B)** Northern blot analysis
99 of PU.1 asRNA in HL-60 cell line using PU.1 as RNA probe after cytoplasmic (c) or nucleic (n)
100 RNA extraction with (+) or without (-) polyadenylation enrichment. U1 snRNA control probe
101 for nucleic RNA extraction enrichment. Ladder legend for RNA size (Kb, kilobase). **(C)**
102 Titration of PU.1 asRNA amplicon (upper panel) and mRNA (lower panel) using the Taqman
103 RT-qPCR assay. Starting DNA at 0.156ng/ μ L (dil1, dilution one) is incrementally diluted at a
104 1:8 ratio (n=2). **(D)** Cell limit determination for PU.1 asRNA and mRNA transcript detection
105 using RT-qPCR assay (green area, lowest cell limit, n=2). **(E and F)** Characterization of **(E)**
106 PU.1 asRNA and **(F)** mRNA transcript quantification with RNase and DNase treatments (n=3)
107 using ssRT-qPCR. **(G and H)** Cell isolation using flow cytometry sorting from healthy donors
108 of **(G)** total bone marrow (HSC-MPP, merged hematopoietic stem cell and multipotent
109 progenitor; CMP, common myeloid progenitor; MEP, megakaryocyte-erythroid progenitor;
110 GMP, granulocyte-macrophage progenitor; LMPP, lymphoid-primed multipotent progenitor;
111 CLP, common lymphoid progenitor) and **(H)** peripheral blood. **(I-K)** Correlation plot between
112 GAPDH housekeeping Ct values from RT-qPCR data and sorted cell number for **(I)** combined
113 hematopoietic stem, progenitor and peripheral blood, **(J)** single populations and **(K)**
114 perturbation experiment in Kasumi-1 cells (Spearman correlation). Data are represented as
115 mean value \pm SEM.

116

117

118

119

120

121

122

123

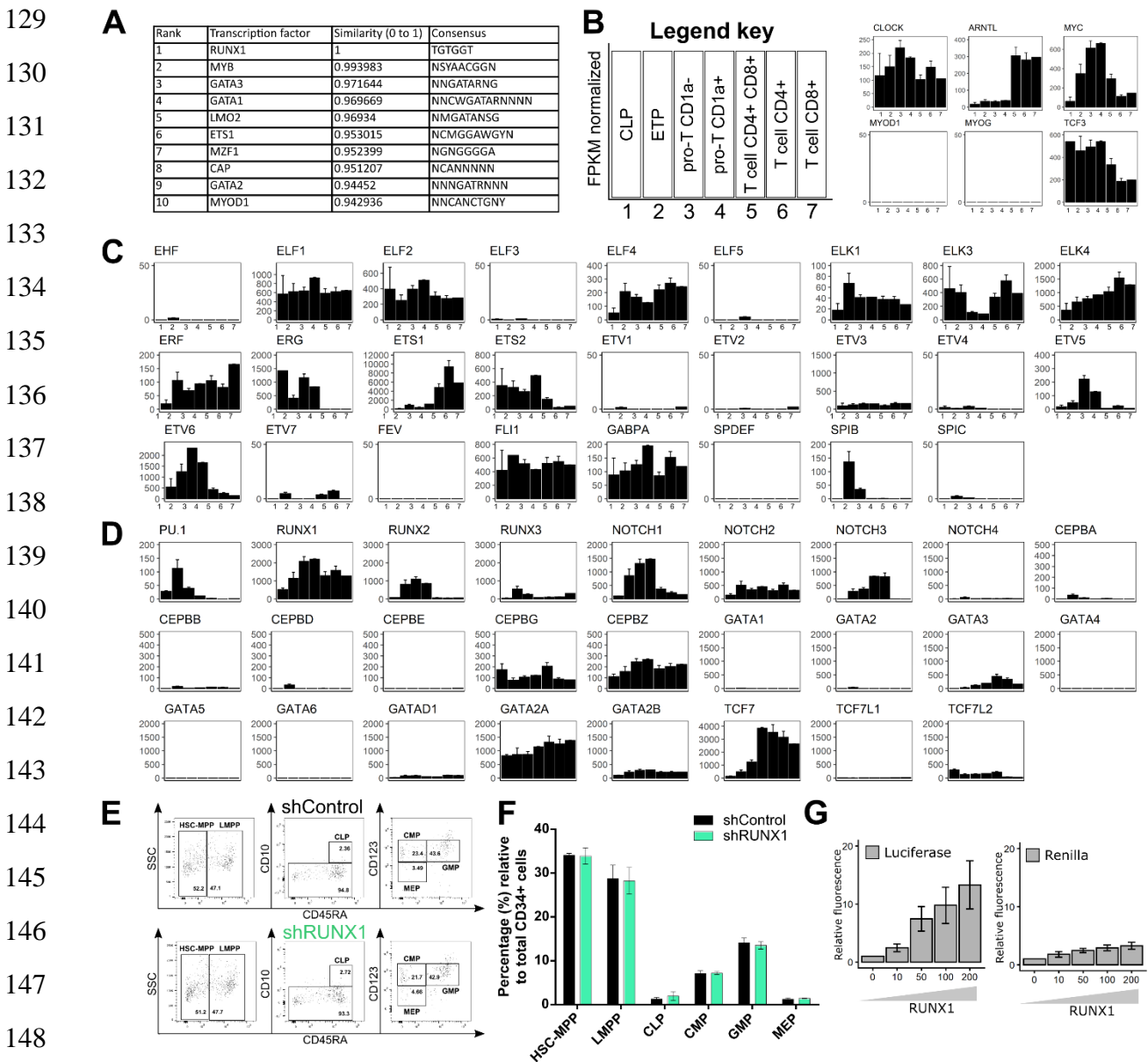
124

125

126

127

128 **Supplemental Figure 2**



144 Supplemental Figure 2. **Early T-lymphoid differentiation regulation by hematopoietic**
 145 **transcription factors.** (A) Ranking for PU.1 antisense promoter (AsPr) transcription factor
 146 binding candidates (TFBind) by similarity (0.0-1.0) between a registered sequence for the
 147 transcription factor binding sites and the input sequence. (B-D) Gene expression by transcript
 148 sequencing (RNA-seq) in thymic progenitors and differentiated T cells (ETP, early thymic
 149 progenitor) for (B) E-box, (C) ETS and (D) most commonly known hematopoietic transcription
 150 factors (RPKM normalized, n=2). (E) Gating of cultivated human HSPCs (HSC-MPP, merged
 151 hematopoietic stem cell and multipotent progenitor; CMP, common myeloid progenitor; MEP,
 152 megakaryocyte-erythroid progenitor; GMP, granulocyte-macrophage progenitor; LMPP,
 153 lymphoid-primed multipotent progenitor; CLP, common lymphoid progenitor). Data displayed

160 as percentage of parent population. **(F)** Hematopoietic populations relative to total CD34+ cells
161 after shRUNX1 (control small-hairpin knockdown against Renilla713, shRen713) in human
162 cultivated HSPCs (n=2). **(G)** Luciferase and Renilla fluorescence measurements relative to 0ng
163 expression plasmid control for PU.1 AsPr Luciferase transactivation in the presence of RUNX1
164 (n=4). Data are represented as mean value \pm SEM.

165

166

167

168

169

170

171

172

173

174

175

176

177

178

179

180

181

182

183

184

185

186

187

188

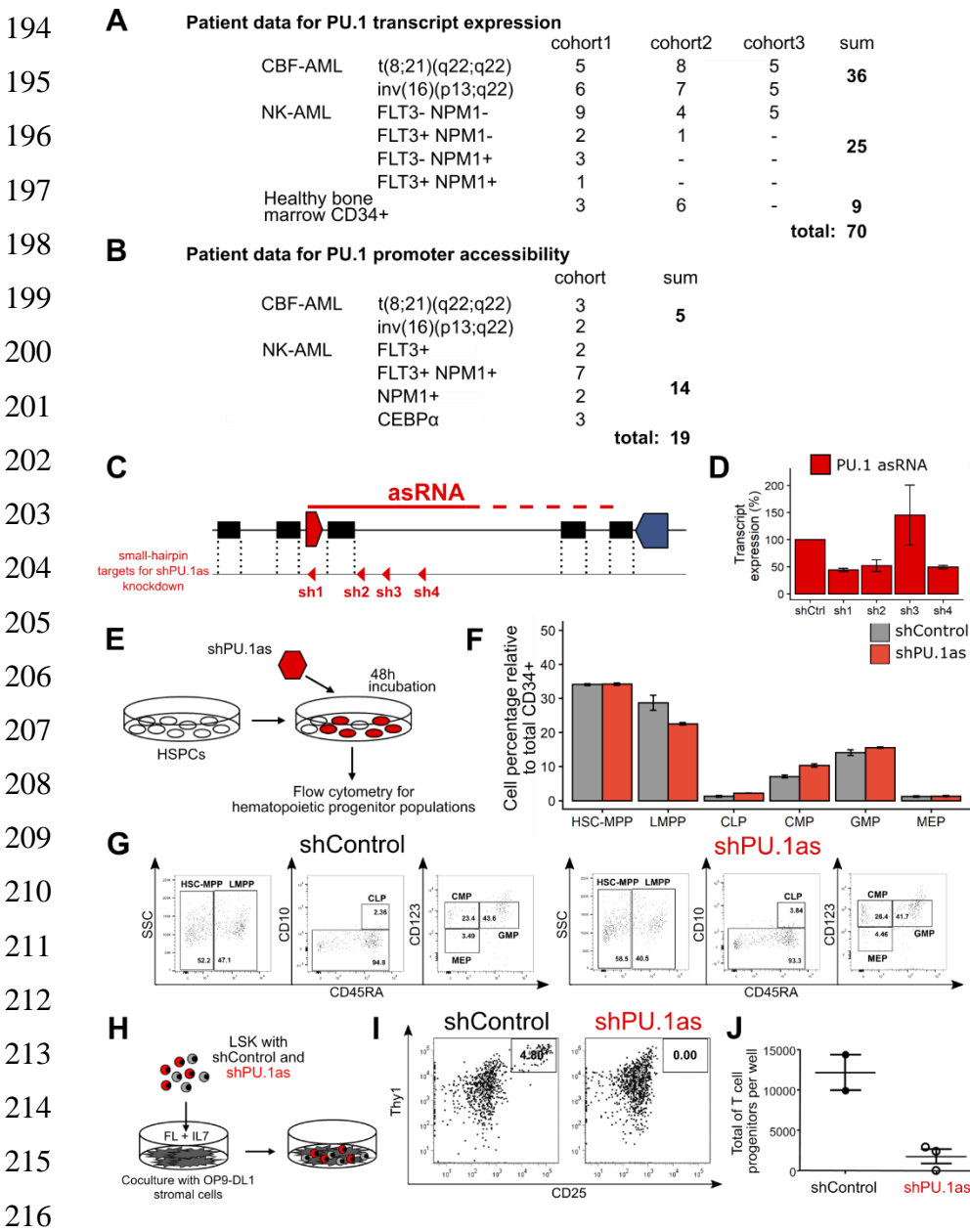
189

190

191

192

193 **Supplemental Figure 3**



217 Supplemental Figure 3. **Validation of PU.1 asRNA depletion in vitro and ex vivo.** (A) Core-
 218 binding factor AML (CBF-AML) patient group for PU.1 transcript expression analysis contains
 219 the t(8;21)(q22;q22) translocation and inv(16)(p13;q22) inversion anomalies, respectively
 220 generating RUNX1-ETO and CBF β -MYH11 fusion proteins, and is subdivided by cohort.
 221 Normal karyotype AML (NK-AML) patient group is subdivided by cohort and by mutation
 222 (Fms-like tyrosine kinase, FLT3; nucleophosmin, NPM1). Bone marrow (BM) CD34+ group
 223 contains healthy CD34-enriched bone marrow samples. (B) CBF-AML patient group for
 224 promoter accessibility analysis (Assi SA, et al. Nat Genet, 2019) contains the t(8;21)(q22;q22)
 225 translocation, inv(16)(p13;q22) inversion anomalies and NK-AML patient group contains
 226 FLT3, NPM1 or CCAAT/enhancer-binding protein alpha (CEBP α) mutations. (C) Schematic

227 representation of the PU.1 locus with the antisense promoter (AsPr, red arrow box) regulating
228 antisense RNA (asRNA, red line). Small-hairpin targets 1 to 4 (sh1-4) for lentiviral knockdown
229 of PU.1 asRNA (shPU.1as, red arrows). **(D)** PU.1 asRNA (red) transcript quantification in
230 Kasumi-1 cells after PU.1 asRNA knockdown (n=2). **(E)** Experimental workflow of shRNA
231 knockdown of PU.1 antisense RNA (shPU.1as) in human hematopoietic stem and progenitor
232 cells (HSPCs) followed by fluorescence-activated cell sorting (FACS). **(F)** Hematopoietic
233 populations relative to total CD34+ cells after shPU.1as (control small-hairpin knockdown
234 against Renilla713, shRen713) in human cultivated HSPCs. **(G)** Gating of cultured human
235 HSPCs (HSC-MPP, merged hematopoietic stem cell and multipotent progenitor; CMP,
236 common myeloid progenitor; MEP, megakaryocyte-erythroid progenitor; GMP, granulocyte-
237 macrophage progenitor; LMPP, lymphoid-primed multipotent progenitor; CLP, common
238 lymphoid progenitor). Data displayed as percentage of parent population. **(H)** Experimental
239 workflow of shRNA knockdown of PU.1 antisense RNA (shPU.1as) in humanized PU.1 LSK
240 (Lin- Sca-1+ c-kit+) mouse cells followed by coculture with OP-DL1 stromal cells for T-
241 lymphoid differentiation. **(I)** FACS analysis for Thy1 and CD25 surface marker expression for
242 T-lymphoid differentiation after shPU.1as in LSK cells and coculture with OP9-DL1. **(J)**
243 Absolute count per well of T-lymphoid progenitors after shPU.1as in LSK cells and in vitro
244 coculture with OP9-DL1.

245

246

247

248

249

250

251

252

253

254

255

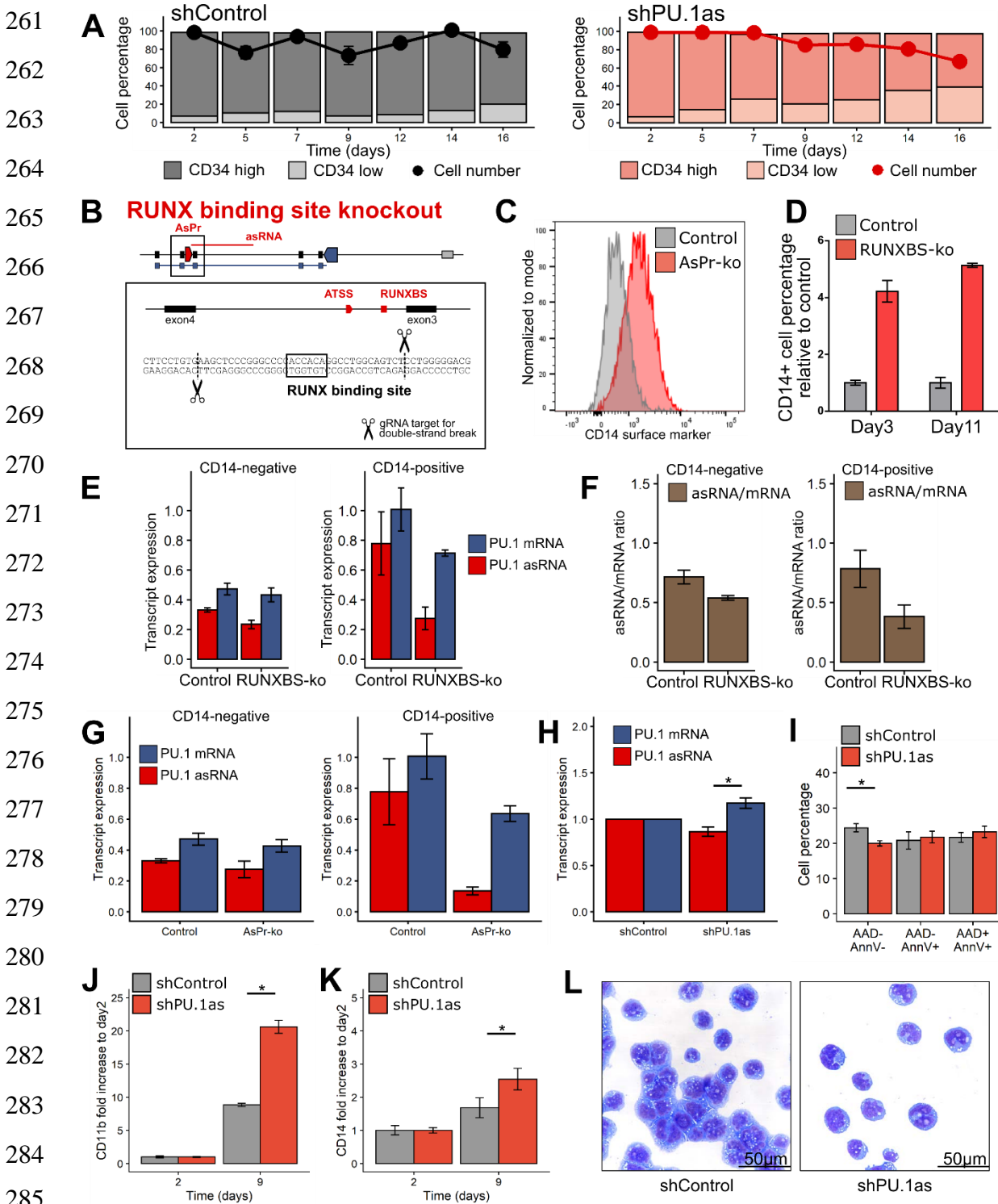
256

257

258

259

260 **Supplemental Figure 4**



286 Supplemental Figure 4. **PU.1 asRNA function assessment in CBF-AML cell lines.** (A) FACS
 287 analysis for CD34 surface marker expression and cell viability kinetics after shPU.1as in
 288 Kasumi-1 (n=4). (B) Schematic representation of the PU.1 locus with the antisense promoter
 289 (AsPr, red arrow) regulating antisense RNA (asRNA, red line) and the double-strand break
 290 locations for CRISPR/Cas9-mediated RUNX binding site (RUNXBS) knockout. Also shown
 291 is the antisense transcription start site (ATSS).

292 expression after RUNXBS knockout (RUNXBS-ko) in Kasumi-1 (merged n=4). **(D)** Kinetics
293 of CD14 surface marker expression after RUNXBS-ko in Kasumi-1 (n=4). **(E)** PU.1 asRNA
294 (red) and mRNA (blue) transcript expression after RUNXBS-ko in CD14-negative and CD14-
295 positive Kasumi-1 cells (n=4). **(F)** PU.1 asRNA/mRNA ratio (brown) after RUNXBS-ko in
296 CD14-negative and CD14-positive Kasumi-1 cells (n=4). **(G)** PU.1 asRNA (red) and mRNA
297 (blue) transcript expression after AsPr-ko in CD14-negative and CD14-positive Kasumi-1 cells
298 (n=4). **(H)** PU.1 asRNA and mRNA (blue) transcript quantification in ME-1 cells after
299 shPU.1as with sh4 (n=3). **(I-K)** Flow cytometry after shPU.1as with sh4 target in ME-1 cells
300 for **(I)** cell viability, **(J)** CD11b and **(K)** CD14 surface markers (n=3). **(L)** May
301 Grünwald/Giemsa cytopins for morphology analysis of ME-1 cells after shPU.1as (n=3). Data
302 are represented as mean value \pm SEM. *p < 0.05, ***p < 0.001, Student's t-test.

303

304

305

306

307

308

309

310

311

312 **Supplemental Figure 5**

313

314

315

316

317

318

319

320

321

322

323

324

325

326

327

328

329

330

331

332

333

334

335

336

337

338

339

340

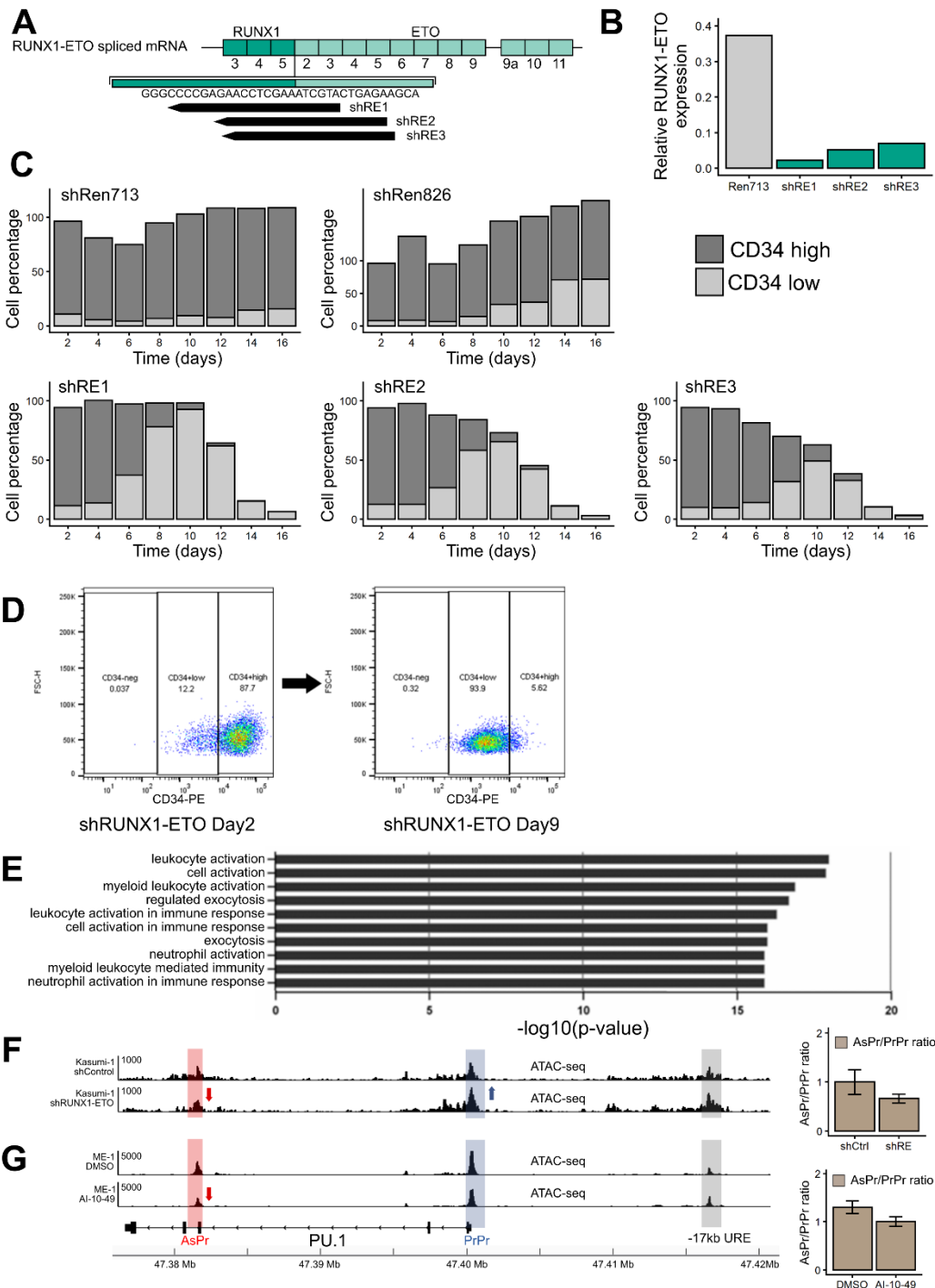
341

342

343

344

345



Supplemental Figure 5. **RUNX1-ETO depletion by lentiviral small hairpin knockdown prevents cell differentiation and myeloid function.** (A) Scheme of shRUNX1-ETO knockdown targets (shRE1-3, small hairpin RUNX1-ETO knockdown for target 1-3). (B) RUNX1-ETO RT-qPCR relative to GAPDH housekeeping gene after RUNX1-ETO

346 knockdown using each shRE target at day10 in Kasumi-1 cells (single replicate). **(C)** CD34
347 surface marker kinetics assessed by flow cytometry for two negative viability controls
348 (Renilla713 and 826, shRen713 and shRen826) and three constructs for RUNX1-ETO lentiviral
349 knockdown in Kasumi-1 cells (single replicate). **(D)** Flow cytometry analysis of CD34 surface
350 marker at day2 and day9 after shRUNX1-ETO (shRE) in Kasumi-1 cells (n=2). **(E)** Top 10
351 Pathway gene ontology analysis using Panther from transcript sequencing (RNA-seq) after
352 shRUNX1-ETO in Kasumi-1 cells (n=3). Differential expression of shRUNX1-ETO Day9
353 compared to shControl Day2-Day9. **(F and G)** URE-adjusted peak quantification values by
354 ATAC-seq for PU.1 antisense (AsPr, red) and proximal promoter (PrPr, blue) exhibited as
355 AsPr/PrPr ratio for **(F)** RUNX1-ETO knockdown in Kasumi-1 cells (2 days after lentiviral
356 transduction, n=3) and for **(G)** AI-10-49 inhibitor treatment of ME-1 cells (6 hours after
357 treatment, n=2). Data are represented as mean value \pm SEM.

358

359

360

361

362

363

364

365

366

367

368

369

370

371

372

373

374

375

376

377

378

379

380 **Supplemental Figure 6**

381

382

383

384

385

386

387

388

389

390

391

392

393

394

395

396

397

398

399

400

401

402

403

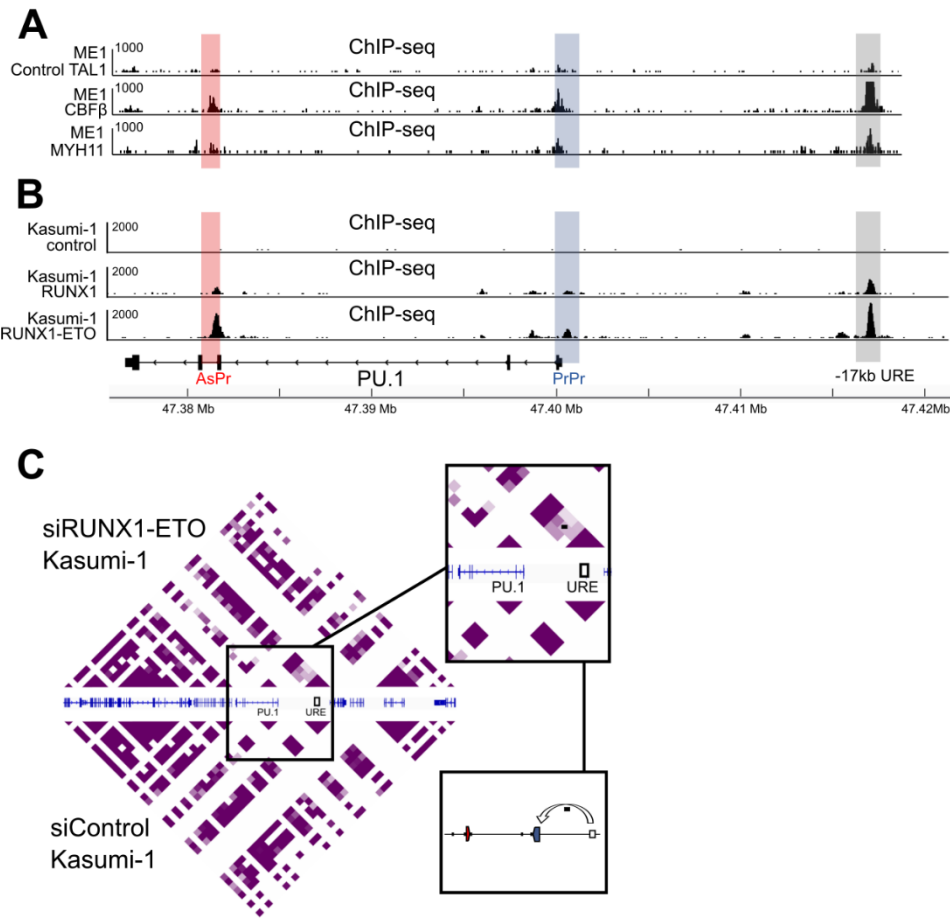
404

405

406

407

408



Supplemental Figure 6. **PU.1 upstream regulatory element is mobilized in early lymphoid differentiation and in PU.1 downregulation by the RUNX1-ETO oncogene.** (A) Chromatin immunoprecipitation sequencing (ChIP-seq) of CBFβ, MYH11 and TAL1 at the PU.1 locus (AsPr, antisense promoter; PrPr, proximal promoter; URE, upstream regulatory element). TAL1 was used as a negative control. (B) RUNX1 and RUNX1-ETO ChIP-seq in Kasumi-1 cells (with immunoglobulin G control, IgG). (C) Promoter capture chromosomal conformation sequencing (C-HiC) after small-interfering RNA of RUNX-ETO knockdown (siRUNX1-ETO) versus control (siControl). Black dot indicates chromosomal looping of -17kb URE and PrPr. Data are represented as mean value ± SEM.